Fracture Characterization of the

Bandelier Tuff in OU-1098 (TA-2 and TA-41)

MASTER

Los Alamos
NATIONAL LABORATORY

An Affirmative Action/Equal Opportunity Employer

Fracture Characterization of the
Bandelier Tuff in OU-1098 (TA-2 and TA-41)

Kenneth H. Wohletz

Los Alamos
NATIONAL LABORATORY

DISCLAIMER

Portions of this document may be illegible in electronic image products. Images are produced from the best available original document.

Fracture Characterization of the Bandelier Tuff in OU-1098 (TA-2 and TA-41)

Kenneth H. Wohletz

ABSTRACT

Rock fracture characterization documents a total of 1496 fractures in unit 2 of the Tshirege Member of the Bandelier Tuff along 6013 feet of Los Alamos Canyon's north wall adjacent to Operational Unit 1098. Geologically termed *joints*, these fractures likely owe their primary origin to brittle failure during the cooling contraction of the tuff after its emplacement nearly 1 million years ago. Subsequent tectonic movement along the Pajarito Fault system has modified fracture strikes, dips, apertures, and linear density. From a background linear density of approximately 20 fractures per 100-foot interval along the canyon wall, fracture density increases to values in excess of 50 fractures per 100-foot interval in a zone at and immediately east of the Omega West reactor building TA-2-1. This increase in fracture density is coincident with the mapped trace of the Guaje Mountain Fault (GMFZ) that apparently bifurcates with a branch running through the canyon at Building TA-2-1 and another about 200 feet east of the Omega site east gate. With it occurs notable slump failure of the canyon wall, increased cumulative fracture aperture, and slight rotation of fracture orientations. Fractures show average strikes of either N35W or N47E, average dips between 75N and 82N, and average apertures of 0.7 cm. Calculations, based on the assumption that fracture apertures are produced by vertical movement along each fracture, suggest approximately 3 m of westward downdrop has occurred over the GMFZ is this area. While fracture character is not documented for Bandelier Tuff units above and below unit 2, observations indicate that inferred tectonic movement has likely influenced fracture permeability in the Bandelier Tuff in Los Alamos Canyon along the trace of the Guaje Mountain Fault. Because of increased fracture permeability, groundwater movement is expected to show greater penetration into bedrock units in that area just east of the Omega West reactor.

INTRODUCTION

The Tshirege (upper) Member of the Bandelier Tuff contains numerous rock fractures throughout its total areal extent, including areas underlying Los Alamos National Laboratory. These fractures are geologically termed *joints* and are a common feature of welded ash-flow tuffs such as the Bandelier Tuff. These fractures are an important and very obvious physical feature of the tuff and play an important role in appraisal of geological features that might affect

environmental remediation studies. First of all, following previous studies of fractured tuff by Barton and Hsieh (1989) and Fuller and Sharp (1992), their presence and abundance are key factors in understanding the vadose-zone hydrology of the Bandelier Tuff and their possible effect on contaminant infiltration from waste disposal areas. In addition, the fractures introduce an increased potential for rock falls from cliffs near laboratory installations (Vaniman and Wohletz, 1990).

Historically, studies of these fractures were undertaken to evaluate their relationship to tectonic fault zones underlying the laboratory areas and the possible seismic hazard to laboratory structures (Vaniman and Wohletz, 1990). This present study builds on that earlier work and complementary work at OU-1106 (TA-21) completed in 1993 (Wohletz, 1995).

The north wall of Los Alamos canyon runs parallel to the northern boundaries of TA-2 and TA-41, areas that comprise Operational Unit (OU) 1098. Units 1, 2, and 3 of the Tshirege Member are exposed in this wall with unit 2 being a prominent cliff-forming unit with nearly continuous exposure of rock fractures (Fig. 1). Field work began in May 1994 and was completed in September 1994. Following the methodology outlined below, the present fracture traverse comprises seven photomosaic maps, constructed to document unit 2 along canyon walls extending 6013 feet from about 975 feet west of TA-41-4 to 1439 feet east of TA-2 (Fig. 2). All locations discussed will be in feet east of the west end of the fracture traverse. Figure 3 is an example of the fracture mosaic maps for the section of cliff exposure adjacent to Omega Site.

METHODOLOGY

The methodology follows three phases of study outlined by the *ER Fracture Characterization SOP* (LANL-ER-SOP-03.06): (1) photographic documentation of area or traverse along which fractures will be characterized, with construction of a photomosaic map base; (2) measurement and plotting of fracture dimensions on the photomosaic map; and (3) statistical analysis of fracture data by procedures described below.

Photo Documentation. In photographing unit two of the Tshirege Member, successive stations at the base of the unit where slopes are accessible were set up such that focal distances of about 40 to 60 feet were maintained and photographs had about 20% overlap. Due to the curvature of the cliff face and its irregular vertical extent, each photograph covered between 30 to 50 feet of lateral exposure; scales added to the photomosaics reflect this variable lateral scale. After construction of the photomosaic, tracing paper was overlaid to make a map of outcrop features including key topographic points such as cliff tops and bottoms, prominent fractures, and geographic objects such as buildings, trees, and large sign posts. This map was attached to the base of the photomosaic such that a one-to-one correspondence can be made between mapped and photographed features. The 6013 foot traverse required 7 individual photomosaic maps.

Fracture Measurement. The horizontal scale for the fracture maps was determined by measuring distance on the topographic map between topographic points identified on the photomosaics. This scale was then placed upon the map to show the distance between mapped features. Because of topographic irregularities of the cliff face described above, this scale will have an error of about ±10% of each map's total width. Starting from one end of the fracture traverse, each fracture was sketched upon the map and designated by a number. These numbers increase from east to west and are pertinent only to the photomosaic map on which they are shown (*e.g.*, fracture numbers 1 through 167 of Fraction Section 3, Fig. 3). Because fracture

Figure 1. Geologic map of the central portion of Los Alamos National Laboratory [see Vaniman and Wohletz (1990) for details], showing the traces of the Rendija Canyon and Guaje Mountain Fault zones, numbered fracture traverses from this and previous studies, and zones of mapped increased fracture density. This report focuses on fracture traverse 4 in Los Alamos canyon, which has an eastward extension in traverse 3 (Wohletz, 1995).
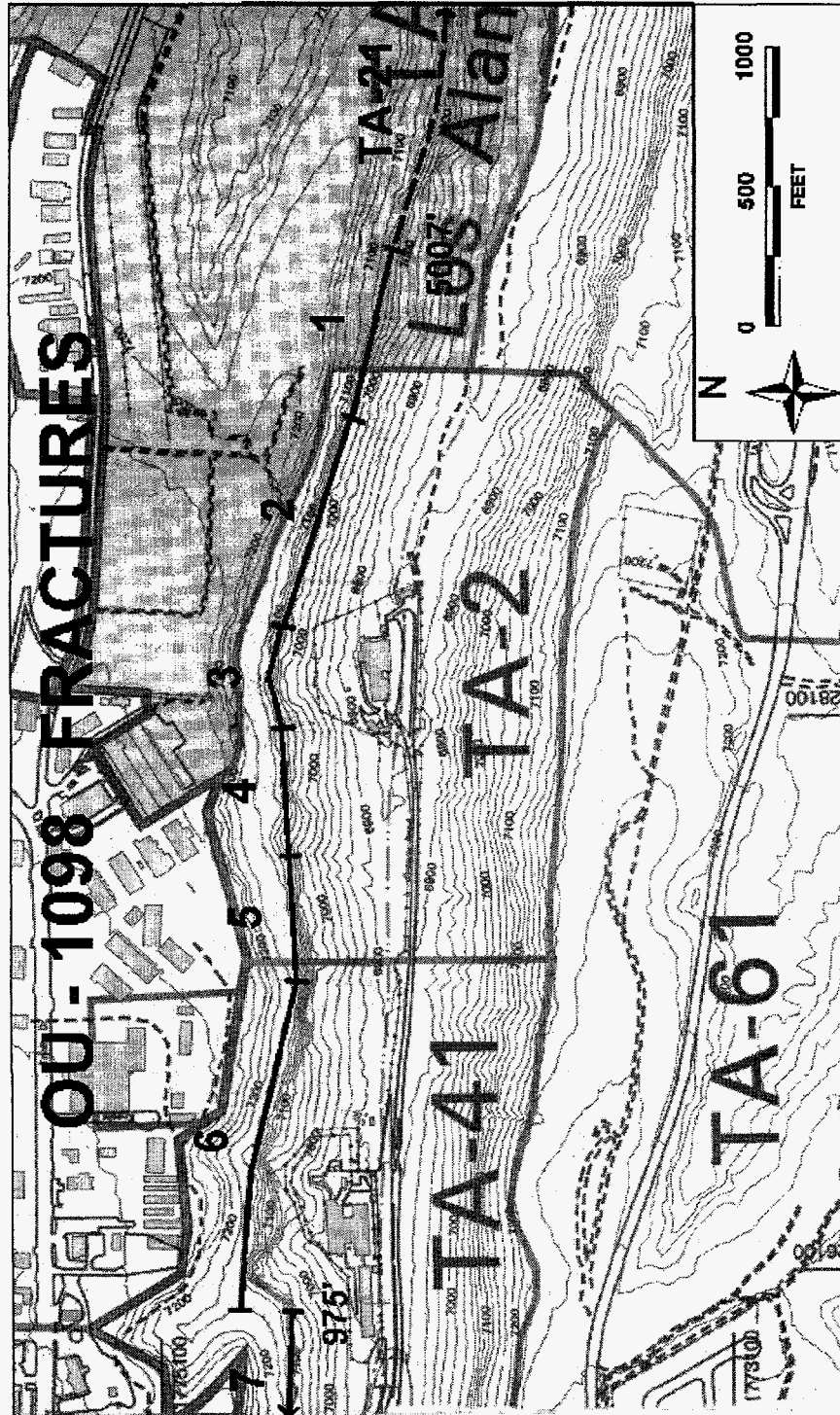
Figure 2. Topographic map of part of Los Alamos canyon along OU-1098 showing the fracture traverse consisting of 7 photomosaic maps of indicated positions. The east end of map 7 is 975 feet from its west end (off the map) and map 1 extends east to 5007 feet. Data from an additional 1000 feet east of map 1 was included in this report from maps 1, 2, and 3 from Wohletz (1995).

Figure 3.   An example fracture photomosaic map (map 3) adjacent to Omega Site (TA-2-1).   Each documented fracture has a number for its identification in the fracture data base.

exposure and accessibility are not ideal for precise measurement, fracture measurements have intrinsic errors of approximately 10 feet in location (at their average point of intersection with the map), 5 degrees in strike and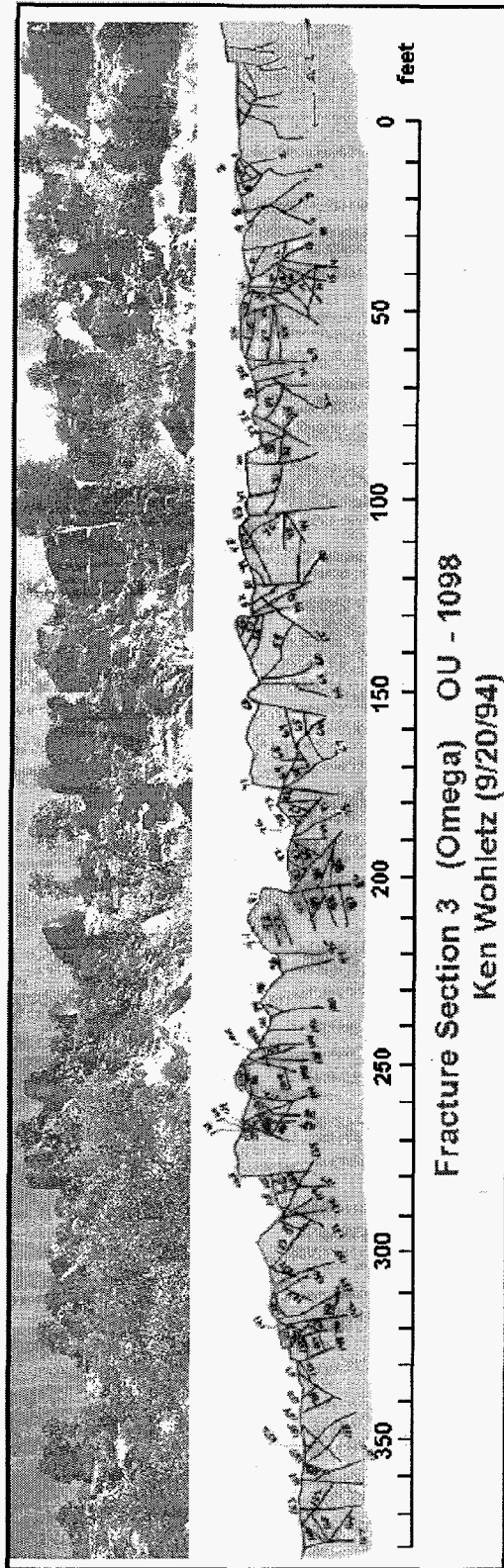 dip (Brunton compass measurement), and 1 cm in aperture (measured perpendicular to fracture surfaces). These errors, however, are similar to the natural variability in individual fracture character (demonstrated on photomosaic maps), each fracture being sinuous and of variable strike, dip, and aperture. In cases where fractures could not be safely accessed, standard Brunton compass techniques were applied, which require measurement using the compass alignment sights with cautious observation of the relationship between true and apparent orientations. All observed fractures have been recorded with some parallel sets too closely spaced to be given individual numbers on the maps, but nonetheless they were recorded in the field notebook.

Fracture Data Base and Analysis. The fracture data recorded in the field notebook were entered into an RS/1 data base, which allowed application of several statistical procedures. The data base consists of a table with a column for each fracture listing the fracture's number designation, its horizontal location shown on the fracture map, its dip and strike, and its width. From these data several other columns are statistically calculated, including: (1) a linear fracture density calculated as a moving average by counting the number of fractures contained in a given distance interval (10 and 100 feet) centered on each fracture; (2) a cumulative fracture aperture over a specified interval (10 and 100 feet) centered on each fracture; and (3) relative dip of fracture from vertical where negative values indicate southerly inclinations. Because fractures in the Bandelier Tuff show apparent NW and NE strike groupings, and cross-cutting relationships suggest that these two groups are coeval, I have considered fractures to represent a conjugate set. Accordingly, additional columns for the table are separately calculated for fracture density, cumulative fracture aperture, and relative dip for each conjugate set. Numerical procedures for the above calculations are: (1) calculation of linear fracture densities for several different distance intervals, taking into account section end effects by extrapolation of the gradient of density with distance; (2) transformation of dip measurements to degrees from vertical; and (3) computation of cumulative fracture widths for 10 and 100 foot distance intervals. While more sophisticated statistical analyses can be applied to these data sets, those used are sufficient to characterize the fractures.

Fracture data were then displayed on several different plots using a LOWESS (Locally Weighted Regression Scatter Plot Smoothing) algorithm to better illustrate data trends. The plots consists of (1) fracture density (100 foot intervals) *vs* horizontal distance along the traverse; (2) rose diagrams of fracture strike; (3) fracture strike *vs* horizontal distance where positive strikes represent strike in degrees east of north and negative strikes are west of north; (4) fracture dips *vs* horizontal distance where vertical plots at zero, dips toward the northeast or northwest are positive inflections from vertical, and southerly dips are negative inflections from vertical; (5) fracture apertures and cumulative fracture widths (per 100 foot interval) *vs* horizontal distance. These plots can show anomalous fracture characteristics in areas of a fault zone (Vaniman and Wohletz, 1990). To better establish trends in fracture data, fractures occurring in inferred fault zones were separated from the data set to allow establishment of relative background fracture character, as discussed below.

FRACTURE CHARACTER

A total of 1496 fractures were documented in the 6013 feet along the north side of Los Alamos Canyon wall adjacent to OU-1098. These fractures are assumed to comprise a conjugate joint set showing general orientation running NW-SE and NE-SW. This result is expected from their origin by cooling contraction of the tuff. Because fractures are documented along a generally E-W line, fractures with strikes near E-W will be underrepresented, which is discussed below in the section on fracture strikes. For purposes of characterization, fractures are grouped according to their strike of NW or NE. As shown below, fracture density increases (anomalies) near Omega Site correspond to the trace of the Guaje Mountain Fault Zone (GMFZ), located between 3200 and 4200 feet on the fracture maps. With this distinction additional grouping includes those fractures in the GMFZ and those east and west of GMFZ in order to establish relative background values. Although the background values discussed below are only pertinent to this area of study, they do show similarity to those discussed by Vaniman and Wohletz (1990) and Wohletz (1995) for other operational units, which lends some credence to their utility.

Fracture Density. Linear fracture density is portrayed in Figure 4 as the number of fractures within a 100-foot interval centered on each fracture for the section starting west of building TA-41-4 and extending 6013 feet down Los Alamos Canyon. From Table 1, fracture density increases from a western background value of 22 fractures per 100-foot interval to over 40 within the GMFZ and then declining to about 30 east of GMFZ. The densities of NW and NE fractures are virtually the same. From previous studies, background fracture densities in the Bandelier Tuff are about 20 fractures per 100-foot interval (Vaniman and Wohletz, 1990; Wohletz, 1995). The value of 30 fractures per 100-foot interval east of the GMFZ likely shows the influence of another fault zone existing near Material Disposal Area V (MDA-V) in TA-21 (~7000 feet east; Wohletz, 1995). Figure 4 shows the prominent rise in fracture density within TA-2 near Omega Site, reaching maximum values between 50 and 60 fractures per 100-foot interval. At 2500 feet another peak in fracture density is apparent. Figure 5 is an enlargement of Figure 4 over the area adjacent to Omega Site building TA-2-1, which likely constitutes a western branch of the Guaje Mountain Fault; the eastern branch exists about 400 feet east of TA-2-1.

Table 1. Fracture Density Data for OU-1098

Fracture Set	Number	Mean Density (#/100 ft)	Standard Deviation (1 σ)
All Fractures	1496	30	±11
NW	709	30	±11
NE	787	30	±11
Background (West)			
NW	308	22	±7
NE	310	22	±7
GMFZ			
NW	194	43	±7
NE	215	42	±8
Background (East)			
NW	207	29	±7
NE	262	28	±6

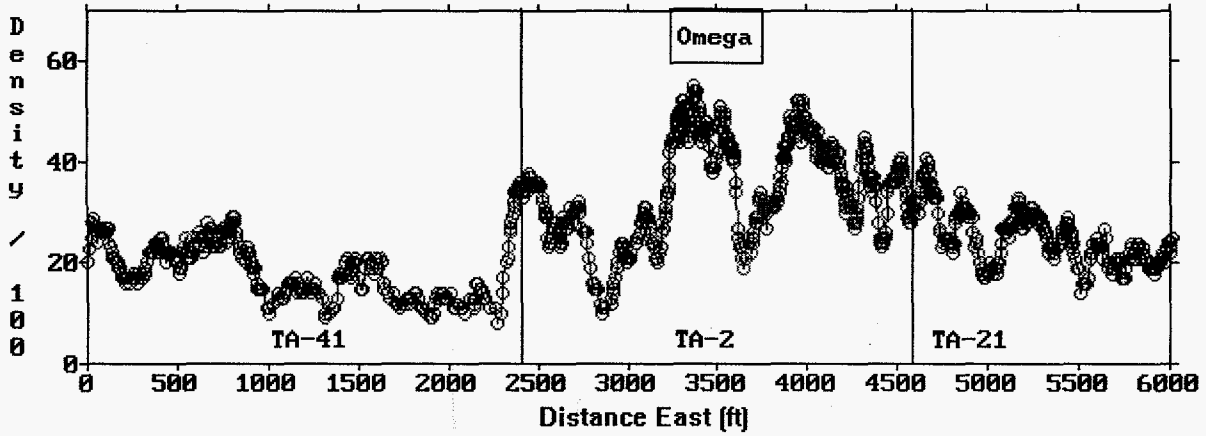**Fracture Density Along Los Alamos Canyon**
(OU — 1098)

Figure 4. Fracture density shows the number of fractures per 100-foot interval centered on each fracture along the traverse of approximately 6000 feet. Note the increase in density from about 3200 to 4200 feet (adjacent to Omega Site), which is the signature of the Guaje Mountain Fault Zone.

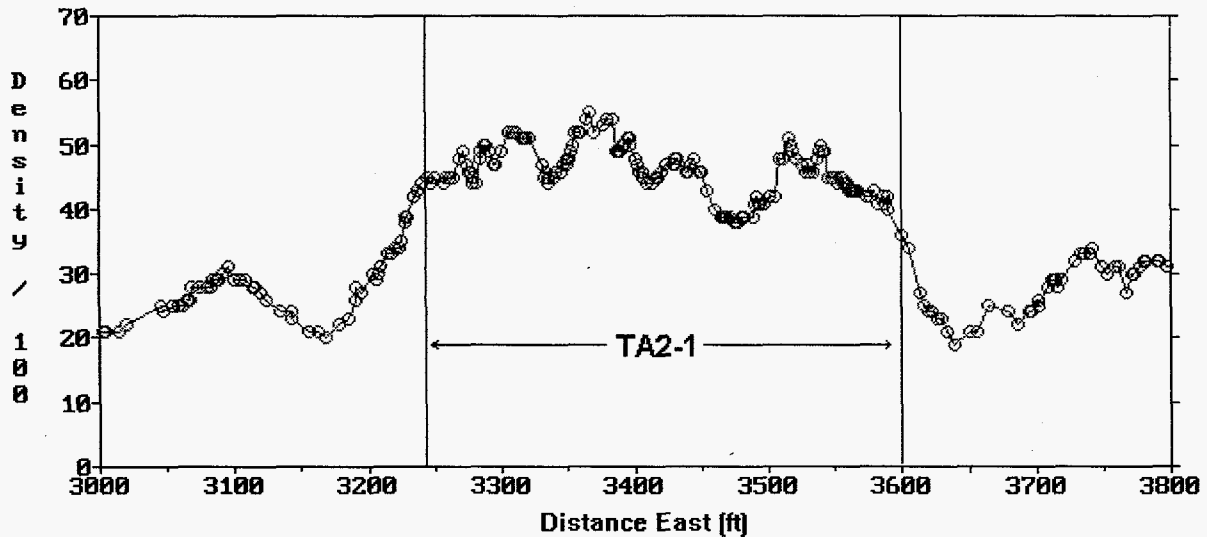**Fracture Density Adjacent to TA2-1**
(Omega West)

Figure 5. Detail of fracture density from 3000 to 3800 feet along the fracture traverse in the region of building TA-2-1 (Omega West reactor).

Fracture Strike. Plotted in a rose diagram (Fig. 6a), fracture strikes show two groupings with mean strikes at N35W and N47E, supporting the conjugate joint-set assumption for distribution of the fractures. As mentioned above, measurement of fractures along a nearly E-W line precludes unbiased representation of fractures nearly parallel to that trend. A compensation algorithm can be defined based on the assumption that the observed fracture abundance is inversely proportional to the cosine of the angle between the fractures and the perpendicular to the line of observation. This algorithm is modified to take into account that the fracture traverse is not a straight line and represents about 20 degrees of variability (canyon wall reentrants allow measurement of some of the fractures striking parallel to the canyon); hence, the maximum compensation will not be infinity but about a factor of 3 [1/(cos 70°)]. Figure 6b is a rose diagram depicting this compensation, which defines a hypothetical but dominant E-W grouping (note that rose diagram depicts E-W trend in bin adjacent to E-W line). The angle between mean strikes is 82° (NW and NE sets) and between 43° (EW and NE sets) and 55° (EW and NW sets).

Table 2 shows the statistical variation in fracture strikes. A subtle increase (6 to 11°) in the angle between NW and NE fractures occurs over the GMFZ compared to background values, but its significance is overshadowed by the dispersion of the strike populations (1 σ = ±20 to±26 degrees), making the effect of the GMFZ on fracture strikes difficult to evaluate. The west to east variation in fracture strike is plotted in Figure 7; the greatest variability is displayed over the GMFZ extending from about 3200 to 4200 feet east, which is the zone of greatest fracture density.
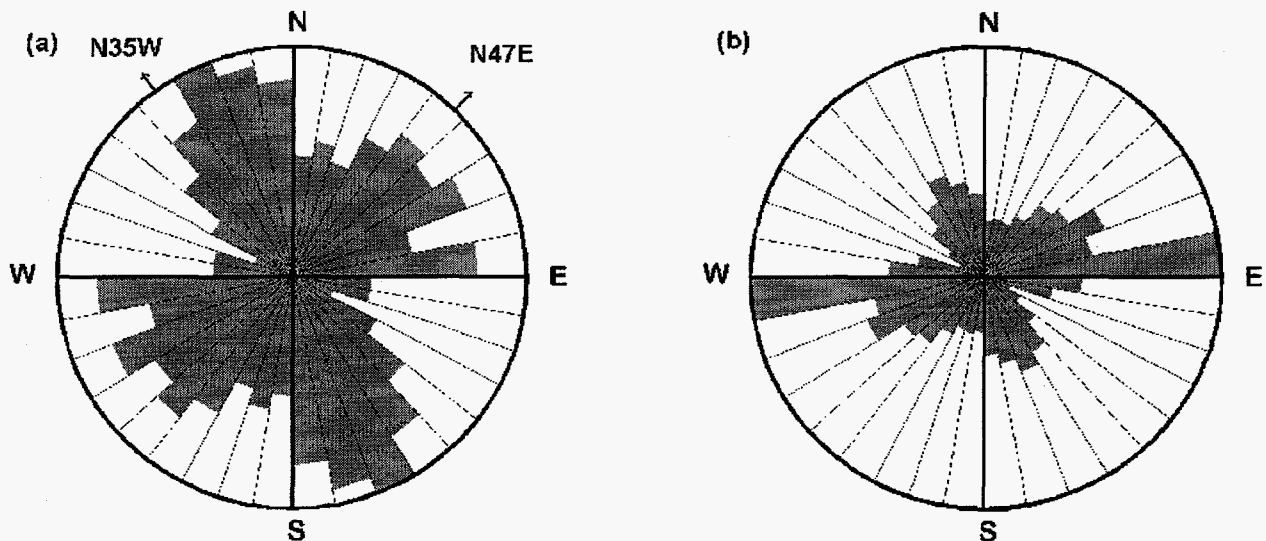

Figure 6. (a) Rose diagram showing the frequency of measured fracture strikes with conjugate set mean values at N35W and N47E. (b) Compensated rose diagram showing hypothetical frequencies of fractures nearly paralleling the fracture traverse.

Table 2. Fracture Strike Data for OU-1098

Fracture Set	Number	Mean Strike (°)	Standard Deviation (1 σ)
All Fractures	1496	N8E	±48
NW	709	N35W	±23
NE	787	N47E	±25
Background (West)			
NW	308	N33W	±20
NE	310	N45E	±26
GMFZ			
NW	194	N38W	±25
NE	215	N51E	±23
Background (East)			
NW	207	N35W	±24
NE	262	N48E	±26

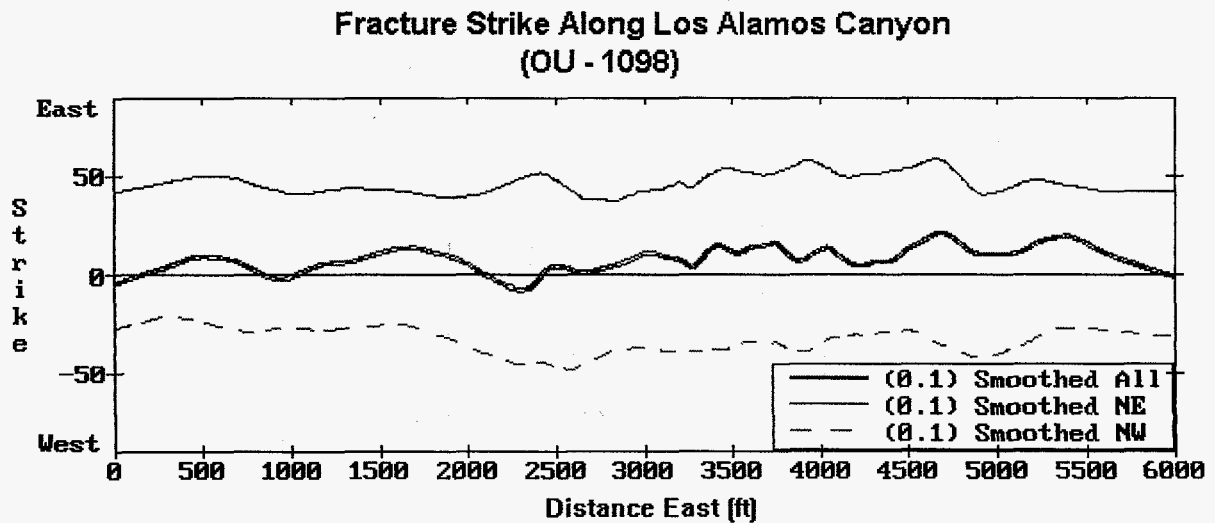**Fracture Strike Along Los Alamos Canyon (OU - 1098)**

Figure 7. Fracture strikes shown as 150 point (0.1) LOWESS (Locally Weighted Regression Scatter Plot Smoothing) curves for all fractures, NE trending fractures (positive values), and NW trending fractures (negative values).

Fracture Dip. Fractures generally dip steeply (Table 3), with mean values near 80° (from horizontal) to the north, attesting that northerly dipping fractures are more abundant than southerly dipping ones. While northerly dipping fractures are steeper than southerly dipping ones for the NW fracture set, they show the same verticality for the NE fracture set (Table 3). The mean dip changes little from background values to those in the GMFZ; however, Figure 8 shows a marked decrease in dip (increase from vertical) for fractures in the regions of high fracture density at ~3400 and ~4100 feet in the GMFZ where the average angle between southerly and northerly dips approaches 70° from a background average of ~35°.

Table 3. Fracture Dip Data for OU-1098

Fracture Set			Number	Mean Dip (°)	Standard Deviation (1 σ)
All Fractures			1496	78N	±33
	NW		709	82N	±32
		N	566	71N	±25
		S	143	58S	±24
	NE		787	75N	±34
		N	636	65N	±29
		S	151	65S	±22
Background (West)					
	NW		308	82N	±28
	NE		310	71N	±36
GMFZ					
	NW		194	78N	±39
	NE		215	71N	±35
Background (East)					
	NW		207	84N	±30
	NE		262	82N	±28

Fracture Aperture. The mean fracture aperture is 0.7 cm (Table 4). This value represents the average opening along the sinuous fractures that in places may be nearly closed and other places open. In unit 2, fracture filling materials were not observed; however, they become abundant in the upper part of unit 3, near the mesa top. In general, the fractures show widest apertures in unit 2 and decrease above and below it, generally being closed in unit 1 where because the tuffs are less competent, fractures are difficult to trace. The mean aperture of fractures slightly increases going east into the GMFZ as shown by Figure 9 and reaches a high value of 1.0 cm at the east of the traverse. Figure 9 also depicts the cumulative aperture over 100-foot intervals centered on each fracture. From background values of about 20 cm of cumulative aperture over 100-foot intervals, values reach about 70 cm of cumulative aperture over the GMFZ. Figure 10 shows the variation of fracture aperture with dip. From this plot, one can see a general increase in fracture aperture as dip goes from 0 (horizontal) to 90 degrees (vertical).

Fracture Dip Along Los Alamos Canyon
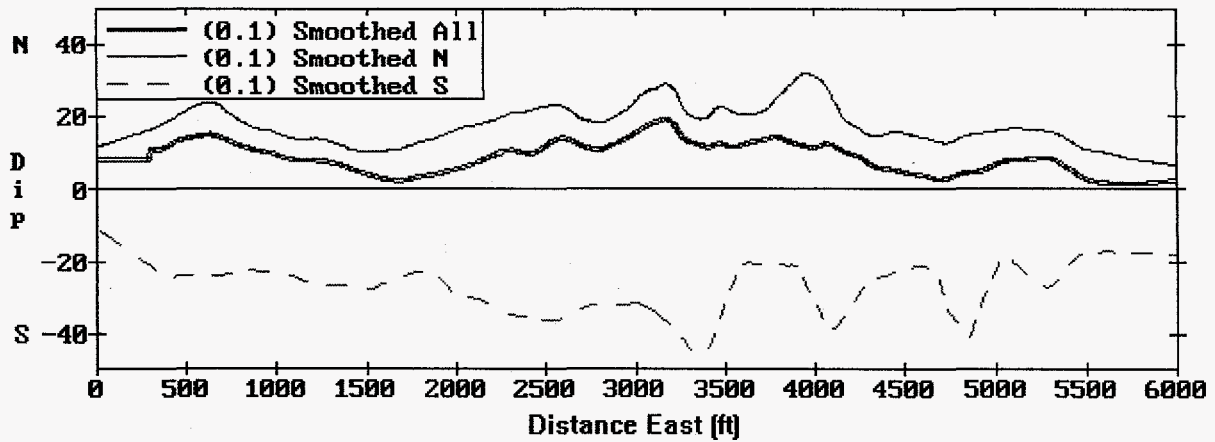## (OU - 1098)

Figure 8. LOWESS (0.1) smoothed curves of fracture dips relative to vertical (0) where southerly dips are shown as negative values. Because there are more north dipping fractures than south dipping ones, the smoothed average of all data shows northerly dipping tendencies.

Table 4. Fracture Aperture Data for OU-1098

Fracture Set	Number	Mean Aperture (cm)	Standard Deviation (1 σ)
All Fractures	1496	0.7	±1.1
NW	709	0.7	±1.1
NE	787	0.7	±1.0
Background (West)			
NW	308	0.6	±0.8
NE	310	0.6	±0.9
GMFZ	409	0.8	±1.3
NW	194	0.8	±1.5
NE	215	0.7	±1.2
Background (East)			
NW	207	0.8	±1.0
NE	262	0.8	±1.1

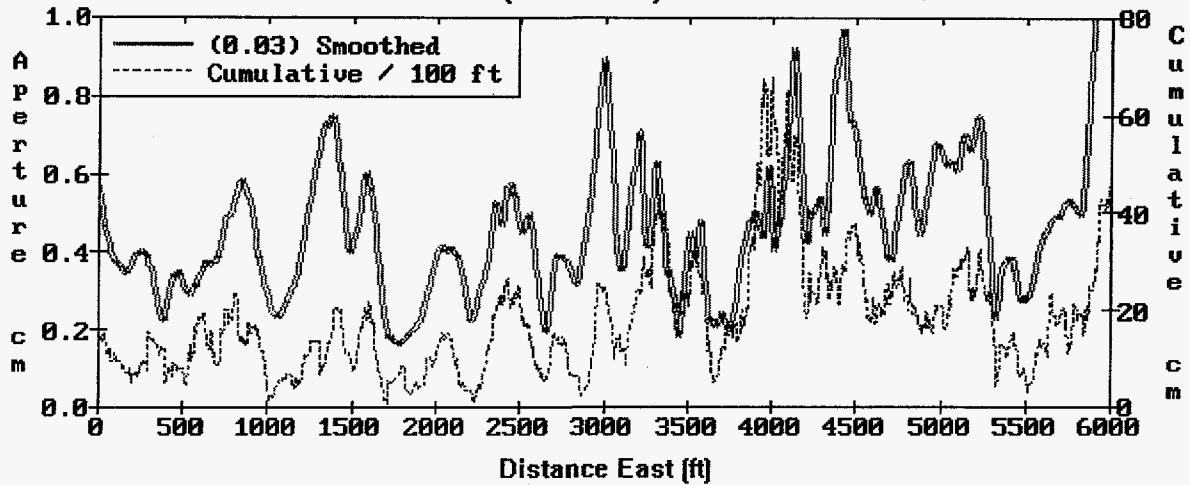## Fracture Aperture Along Los Alamos Canyon
(OU - 1098)

Figure 9. LOWESS (0.03; 45 point) smoothed curve of fracture apertures and the curve for cumulative fracture aperture per 100-foot interval centered on each fracture. The cumulative curve shows peak values in the region of the GMFZ.

Fracture Aperture as Function of Dip
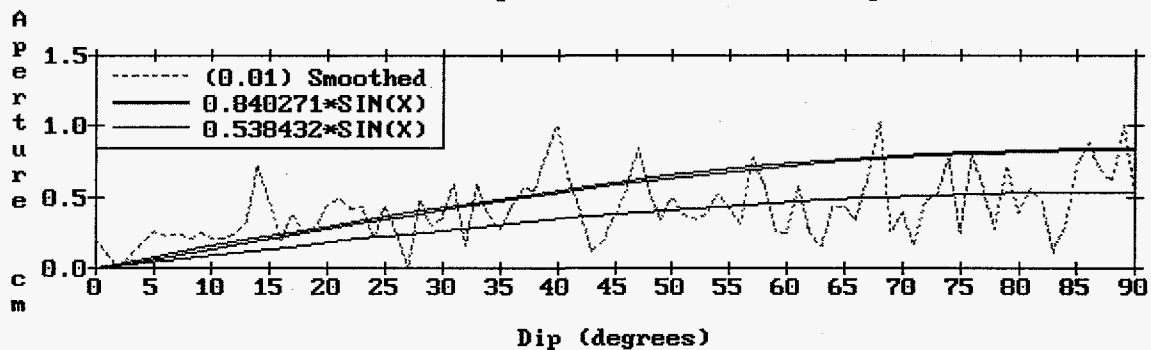
Figure 10. LOWESS (0.01) smoothed curve (dotted) of fracture apertures as a function of dip. Sine curves are shown for a best fit of all aperture data (double) and best fit of smooth data (single). This plot shows that there is a general observed increase in fracture aperture with increasing fracture dip, such that horizontal fractures generally show little or no aperture while vertical ones generally show apertures of about 0.8 cm.

DISCUSSION

The data presented above suggest that observed fractures in the Tshirege Member have origins from both cooling contraction of the tuff during and after its emplacement and subsequent adjustment of the tuff to tectonic movement along the Guaje Mountain Fault Zone. The following discussion presents some interpretations and conclusions regarding (1) fracture geometry; (2) fracture origins; and (3) hydrologic effects of fractures in the Bandelier Tuff.

Fracture Geometry. While DeGraff and Aydin (1993) show that cooling contraction fractures show spacing inversely proportional to cooling rates, the observed increase in Bandelier Tuff fracture density (decrease in spacing) over the GMFZ can also be explained by two tectonic interpretations. (1) Tectonic displacement is accommodated by preexisting fractures and incrementally dispersed over a wide area. In this area, the greater number of fractures derives from tectonic stresses opening new cracks along zones of weakness or incipient fractures originally caused by cooling contraction. (2) A tectonic fracture pattern overprints the preexisting cooling fractures. Both interpretations can be supported in that (1) it is difficult to find evidence of significant displacement along most fractures in the form of offset lithologies, but (2) there are common structural features along fault traces such as *micrograbens* and *zipper joints* that suggest downdrop of individual blocks of tuff in isolated areas near the top of unit 2 (Vaniman and Wohletz, 1990). A consideration, discussed by DeGraff and Aydin (1993), is that convective movement of fluids in fractures will increase the overall cooling rate resulting in more closely spaced fractures. In that light, one might also suppose that the increased fracture density areas represent areas of convective cooling in the tuff, but increased occurrences of fumarolic pipes and vapor-phase alteration, which result from such cooling, have not been documented.

If in fact tectonic displacement has been accommodated by the 409 documented fractures over the GMFZ (3200 to 4200 feet) by incremental, vertical displacement on each fracture, then with summation of these displacements one can test the model of Gardner and House (1987) that shows downdrop on the west side of this fault zone. Because most fractures do not show measurable evidence of incremental displacement, an alternative method is proposed here, a method based on the assumption that fracture apertures have developed by vertical displacement along initially closed cooling joints. Figure 11 illustrates this method, showing how a vertical displacement along a fracture produces a fracture aperture where the apparent downdrop equals the aperture divided by the cosine of the dip. This method also requires the assumption that vertical fractures produce no aperture, which is incorrect considering observed data (Fig. 10); however, if vertical fractures were included in this method, then an infinite vertical displacement would arise, which is obviously incorrect. Furthermore, cooling contraction of the tuff may have produced fracture apertures, but I note that many localities in the Bandelier Tuff show cooling joints having no aperture. Keeping in mind the above assumptions, an application of this method (Figs. 12 and 13) does show an apparent cumulative downdrop of approximately 3 m (10 ft) to west has been accommodated by fractures in this zone. In support of this calculation, Vaniman and Wohletz (1990) calculated ~2 m of vertical displacement on the GMFZ where it crosses East Jemez Road to the south of Los Alamos Canyon. In addition this former study noted an inflection of the Los Alamos Canyon stream gradient of about 20 feet over the GMFZ, which is a common geomorphic feature of fault displacement.

Fracture strikes indicate the presence of a conjugate fracture set with mean trends of N35W and N47E, which is similar to published work on welded tuff (Fuller and Sharp, 1992). Mathematical compensation for the biasing caused by measurement along a nearly E-W line suggests the possible existence of a dominant E-W fracture trend, which supplements the NW and NE fracture groups. At this point, there are no studies that can support this hypothesis, its reality can only be tested where fracture traverses are measured along a N-S line. Such traverses might be done at the east end of mesas, but as of yet such locations where fractures are well exposed have not been located. On the other hand, traverses could be measured on man-made exposures in the Bandelier Tuff in the vicinity of Los Alamos Canyon, if they were constructed.
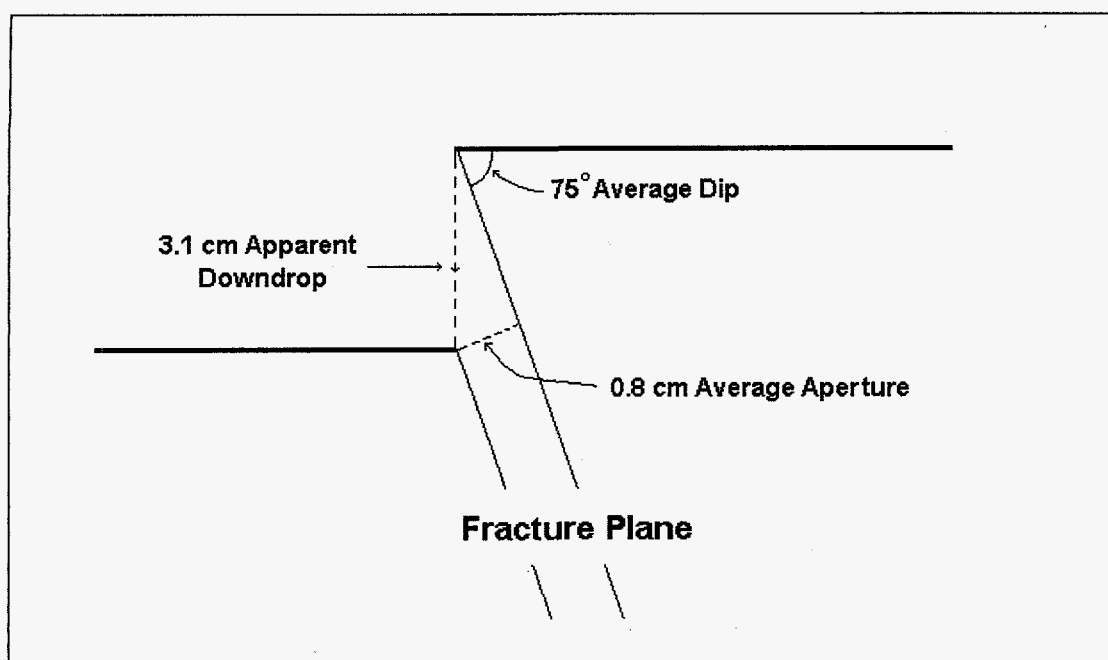
Figure 11. Schematic illustration of average fracture geometry, showing one possible geometric configuration that explains fracture aperture by downdrop of tuff block on the left relative to the one on the right.

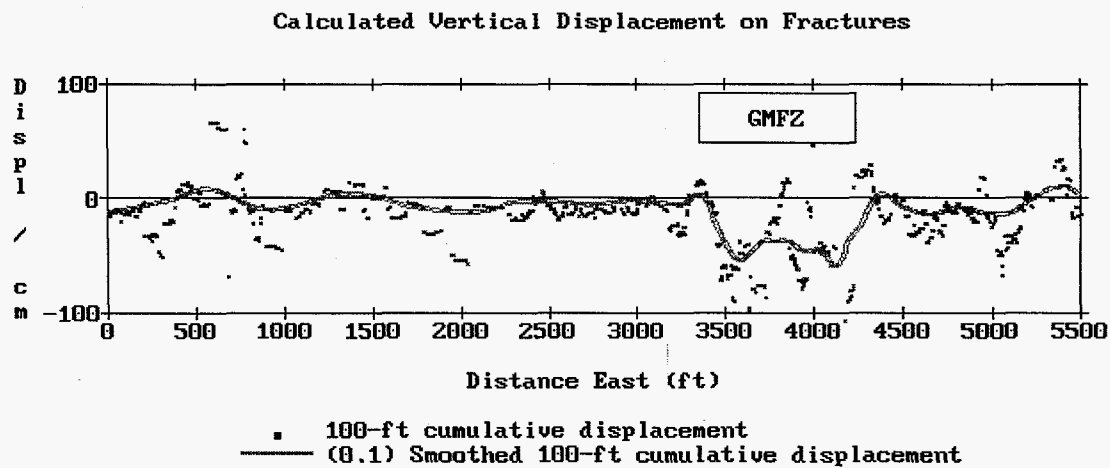**Calculated Vertical Displacement on Fractures**

Figure 12. Fracture aperture per 100-foot interval (interval centered on each fracture) and LOWESS (0.1) smoothed curve of these data calculated as shown in Figure 11. Note the negative (down to the west) signature over the GMFZ between 3200 and 4200 feet.

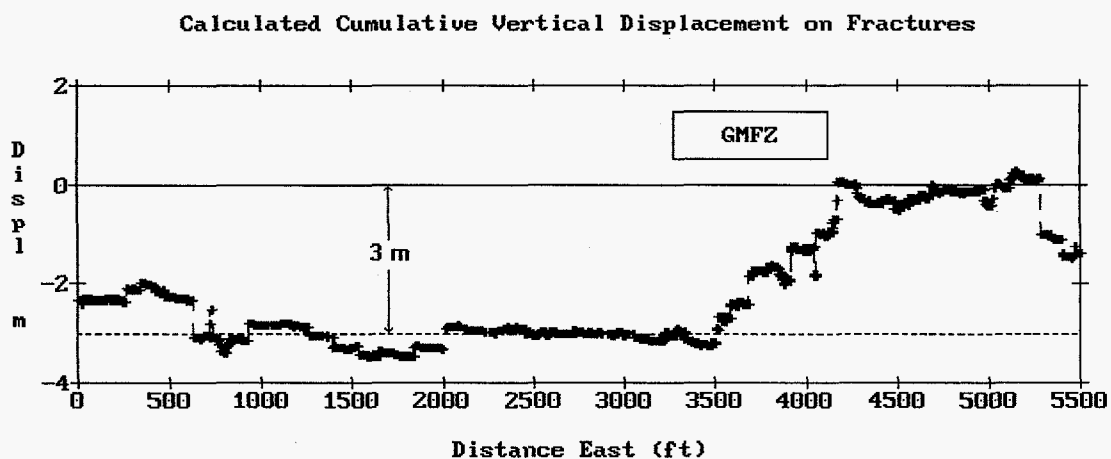**Calculated Cumulative Vertical Displacement on Fractures**

Figure 13. Cumulative fracture vertical displacement calculated as shown in Figure 11. Note the apparent westward downdrop over the GMFZ. Approximately 4m of apparent displacement occurs between 3500 and 4200 feet, where cumulative offset is taken from an arbitrary zero level east of the GMFZ.

Fracture Origins. The origin of conjugate joints can be attributed to cooling contraction of the tuff after its emplacement. While such an origin hypothetically produces a 60° angle between fracture sets in an isotropic medium, existence of stress anisotropy will cause deviations from the 60° angle (MacDonald, 1975). Such anisotropy might have arisen if tuff cooling and compaction occurred over a pre-Tshirege topography consisting of canyons and mesas, which is supported by mapped thinning of the tuff over mesa tops from greatest thicknesses in canyons (Smith et al., 1970), then compaction over canyon walls would produce a dominant N-S flexure with strain accommodated by E-W trending fractures, which would help explain the observed angle between the documented fracture sets.

The observed steep dip on most fractures is predicted by models of the growth of cooling contraction joints (DeGraff and Aydin, 1993). Assuming the tuff to be initially homogeneous and subjected to isotropic stresses prior to cooling compaction, fractures should develop and propagate normal to evolving isotherms during cooling. Such a model crudely predicts the observed pattern of steeply dipping fractures. Fracture dips are dominantly to the north. This observation can be explained by the proximity of unit 2 to a possible pre-Bandelier topographic surface, which was also a north canyon wall. If fractures propagate during cooling contraction normal to isotherms and the isotherms parallel the cold substrate, then fractures would be expected to develop with a northerly dip in this region.

In contrast to fracture aperture data reported by Wohletz (1995), which shows a marked rise in average aperture from background values of ~0.7 cm to ~1.3 cm over the fault zone (with smoothed peak values reaching 3.5 cm), the data for GMFZ show only a slight rise of 0.1 cm above background (with smoothed peak values reaching 1.0 cm). Another contrast of the GMFZ to the fault zone described at TA-21 is that smoothed aperture values fall off by a factor of about two over GMFZ from the high values on either side of it. This observation likely reflects the effects of mass wasting caused by slump failure of the cliffs above TA-2-1. Block rotation caused by the slumping may have decreased the fracture apertures in this zone. Another explanation is that the slumping has exposed the fractures further back in the mesa where they are narrower. If the latter explanation is correct, then fracture apertures measured along canyon walls might be twice that of apertures under the central portion of the mesa. Taking into account fracture measurements from other portions of the laboratory, which show average background apertures along canyon walls to be from 0.6 to 0.7 cm, one might conclude that drilling away from canyon walls in the vicinity of TA-2 would intersect fractures with average apertures of about 0.3 cm.

Hydrologic Effects. A review of tuff hydrology is given by Wood and Fernandez (1988), who compile tuff data from a variety of sources. Fuller and Sharp (1992) show that the existence of fractures in tuff strongly controls effective rock permeability. In addition, fractures in tuff have been characterized at Yucca Mountain in recognition of their role on hydraulic response (Barton and Hsieh, 1989; Barton and Larsen, 1985). From the conclusions presented above, the fracture characterization of OU-1098 suggests that fractures in the Bandelier Tuff below the Los Alamos Canyon floor near TA-2 are more closely spaced and perhaps have a slightly greater aperture than the tuff encountered up canyon from TA-2. This result likely reflects the presence of the GMFZ, which in turn suggests a perturbation of the local hydrology of the canyon. One hydrological effect may be the a greater penetration depth of surface water from runoff and the canyon stream (Fuller and Sharp, 1992). If such increased penetration has occurred over time, then one might expect to find greater development of tuff alteration products (e.g., clays and

zeolites) in the tuff below and adjacent to TA-2 (1994 drilling of borehole LAOI(A)1.1 showed clay zones in the Bandelier Tuff). This reasoning then suggests two endmember possibilities for groundwater infiltration: (1) the increased fracture permeability has enhanced infiltration; and (2) development of tuff alteration materials has partly or completely sealed fractures producing a lower permeability in the region, thus decreasing infiltration. With regards to the former possibility, Fuller and Sharp (1992) demonstrated that the presence of "weathering" (fracture coatings) on tuff surfaces decreases its surface permeability by an order of magnitude. This effect reduces the degree of water interchange between fractures and the tuff matrix and allows a high degree of deep infiltration. In support of the latter interpretation, fractures observed within several tens of feet from mesa tops generally contain fill materials including infiltrated detritus, gypsum, and likely clays and zeolites, while at greater depth in Tshirege Member, fractures are generally open (Vaniman and Wohletz, 1990).

CONCLUSIONS

In documentation and measurement of 1496 fractures in unit 2 of the Tshirege Member along Los Alamos Canyon adjacent to OU-1098, prominent increases in fracture density are found to exist near Omega Site, reflecting the existence of the Guaje Mountain Fault Zone in that area. In general the area of increased fractures extends from 3200 to 4200 feet east along the documented fracture traverse. The variation in fracture density in this zone suggests that the Guaje Mountain Fault is bifurcated into two branches separated by about 700 feet. While the western branch runs directly under building TA-2-1 (Omega West reactor), the eastern branch runs about 200 feet east of the down-canyon gate at Omega Site, near the site of borehole LAOI(A)1.1. Another peak in fracture density occurs at about 2500 feet (near the boundary between TA-41 and TA-2) possibly reflects a fault branch between the Guaje Mountain and Rendija Canyon faults, running WNW into a canyon wall reentrant just north of building TA-41-4.

While fractures producing cliff instability near Omega Site are a risk to present installations in the canyon, the occurrence of fractures with average spacing of 0.6 m and apertures of 0.8 cm in the GMFZ does point to a greater likelihood of groundwater infiltration near Omega Site. How much and to what depth infiltration has affected the canyon below Omega Site might be constrained by hydrologic models such as FEHM (EES-5) using data from this report.

REFERENCES

Barton, C. C. and Hsieh, P. A., 1989, Physical and hydrologic flow properties of fractures. Int. Geol. Cong., 28th, Field trip guidebook T385, 36 pp.

Barton, C. C. and Larsen, E., 1985, Fractal geometry of two-dimensional fracture networks at Yucca Mountain, southwestern Nevada. In: Fundamentals of Rock Joints: International Symposium, Bjorkliden, Sweden, Proc. p. 77-84.

DeGraff, J. M. and Aydin, A., 1993, Effect of thermal regime on growth increment and spacing of contraction joints in basaltic lava. J. Geophys. Res., v. 98, no. B4, p. 6411-6430.

Fuller, C. M. and Sharp, J. M. Jr., 1992, Permeability and fracture patterns in extrusive volcanic rocks: Implications from the welded Santana Tuff, Trans-Pecos Texas. Geol. Soc. Amer. Bull., v. 104, p. 1485-1496.

Gardner, J. N. and House, L., 1987, Seismic hazards investigations at Los Alamos National Laboratory, 1984-1985. Los Alamos National Laboratory report LA-11072-MS, 76 pp.

MacDonald, G. A., 1975, Volcanoes, Prentice-Hall, Inc., Englewood Cliffs, NJ, 510 pp.

Smith, R. L., Bailey, R. A., and Ross, C.S., 1970, Geologic map of the Jemez Mountains, New Mexico. U.S. Geol. Surv. Misc. Geol. Invest. Map, I-571.

Vaniman, D. and Wohletz, K., 1990, Results of geological mapping/fracture studies: TA-55 area. Los Alamos National Laboratory Seismic Hazards Memo EES1-SH90-17, 25 pp, 3 Plates, 23 figures.

Wohletz, K. H., 1995, Measurement and analysis of rock fractures in the Tshirege Member of the Bandelier Tuff along Los Alamos Canyon adjacent to TA-21. In: Earth Science Investigations for Environmental Restoration—Los Alamos National Laboratory Technical Area 21 (DE Broxton and PG Eller, eds), Los Alamos National Laboratory report LA-12934-MS, 19-31.

Wood, W. W. and Fernandez, L. A., 1988, Volcanic rocks. in The Geology of North America, Volume O-2, Hydrogeology, Boulder, Colorado, Geol. Soc. of Amer., p. 353-365.